Communications in Mathematics and Applications
Vol. 16, No. 3, pp. 1–15, 2025
ISSN 0975-8607 (online); 0976-5905 (print)
Published by RGN Publications
DOI: 10.26713/cma.v16i3.2970

http://www.rgnpublications.com

Research Article

Early Detection of Melanoma: Deep Learning and *m*-Health for Optimized Patient Outcomes

Md. Moddassir Alam

Department of Health Information Management and Technology, College of Applied Medical Sciences, University of Hafr Al Batin, Hafr Al Batin 39524, Saudi Arabia
mmalam@uhb.edu.sa

Received: December 25, 2024 **Revised:** March 16, 2025 **Accepted:** April 2, 2025

Abstract. Melanoma, an aggressive skin cancer, claims 57,000 lives annually worldwide. Early detection improves survival rates, reduces mortality, enhances treatment outcomes, increases awareness and provides economic benefits. However, detection faces challenges, including limited dermatologist availability, geographical constraints and inaccurate self-assessment. This study proposes an intelligent *m*-Health system using Squirrel Search Stochastic Gradient Descent (SSSGD) with Deep Quantum Neural Network (DQNN). The SSSGD is the integration of Squirrel Search Algorithm (SSA) and Stochastic gradient descent (SGD). Here, Type-2 Fuzzy and Cuckoo Search-Based Filter (T2FCS) is used for pre-processing Enhance image quality, resize, and normalize. Spine Generative Adversarial Network (Spine GAN) lesion segmentation, geometric transformations data augmentation, Grey Level Co-occurrence Matrices feature extraction, and DQNN detection trained by SSSGD, providing clinicians with a reliable Decision Support System (DSS) for early diagnosis and effective treatment, enhancing accuracy, computational efficiency, and patient outcomes. Performance evaluation metrics include loss curves, confusion matrix, sensitivity (98.61%), specificity (98.13%) and accuracy (98.42%). Results demonstrate enhanced performance, providing clinicians with a reliable DSS for early diagnosis and effective treatment.

Keywords. *m*-Health, Melanoma detection, Deep Quantum Neural Network, Type-2 Fuzzy and Cuckoo Search-Based Filter, Stochastic gradient descent

Mathematics Subject Classification (2020). 68T07

Copyright © 2025 Md. Moddassir Alam. *This is an open access article distributed under the Creative Commons Attribution License, which permits unrestricted use, distribution, and reproduction in any medium, provided the original work is properly cited.*

1. Introduction

Melanoma, an aggressive form of skin cancer, can rapidly spread and metastasize to other organs if left untreated. Primarily affecting sun-exposed areas, skin cancer claims two lives every hour (Thanka *et al*. [24]). The exact cause of skin cancer remains unknown, but prolonged exposure to ultraviolet (UV) rays, pollution, and excessive cosmetic use are potential risk factors (Aljohani and Turki [3], Trager *et al*. [23]). Individuals under 40, especially women, are disproportionately affected. Early detection is crucial, as melanoma is highly treatable in its initial stages, with a high recovery rate (Thanh *et al*. [21]). Warning signs include sudden changes in skin pigmentation, unusual growths, or modifications to existing moles. Melanoma's aggressive nature and tendency to metastasize make timely diagnosis and treatment essential. Prompt medical attention is critical to prevent advanced stages and improve survival rates (Mishra *et al*. [13]). To mitigate this risk, proactive measures are essential, including regular skin examinations and reduced sun exposure. Fortunately, mobile health (m-Health) applications have emerged as a valuable tool in melanoma diagnosis, harnessing artificial intelligence (AI) and machine learning (ML) to analyze skin lesions (Javaid *et al*. [11]). Additionally, m-Health applications increase accessibility to melanoma screening, particularly in resource-constrained settings (Araújo *et al*. [5]). Early melanoma detection poses challenges due to visual similarities between malignant tumors and benign moles, even for experienced doctors (Darmawan *et al*. [8]).

Despite expert dermatologists' expertise, human error can occur, leading to misdiagnosis and potentially life-threatening consequences (Barata *et al*. [7]). To mitigate this, computer-aided diagnosis (CAD) systems leveraging image processing and machine learning techniques have been proposed. These systems analyze dermoscopic images, supporting dermatologists in early decision-making and reducing misdiagnosis. Dermatologists rely on clinical diagnosis rules, including: ABCDE rule (Alquran *et al*. [4]) (Asymmetry, Border, Color, Diameter, Evolve), Seven-point checklist, and Menzies method (Nasr *et al*. [16]). Traditional ML techniques require manual feature extraction, a time-consuming and challenging process (Murugan *et al*. [14]). This project aims to create an m-Health application using deep learning techniques for melanoma diagnosis, improving early detection accuracy and reducing misdiagnosis among dermatologists. The key contributions of this research are as follows.

A DQNN architecture is developed for melanoma detection, utilizing quantum computing principles for improved feature extraction, scalability, and efficiency in processing large medical datasets. The introduction of a hybrid optimization algorithm, SSSGD, combines SSA and SGD for adaptive learning rate strategies, enhancing convergence and accuracy in DQNN parameters optimization. Experiments show SSSGD's effectiveness in converging DQNN weights, outperforming traditional optimization algorithms in convergence rates and accuracy, demonstrating its potential for efficient deep learning optimization. The integration of DQNN and SSSGD improved melanoma detection accuracy, demonstrating enhanced computational efficiency and robustness in processing diverse datasets.

The remainder of this paper is structured as follows: Section 2 elaborates on prevailing methodologies and their challenges, Section 3 describes the m-Health system model, Section 4 details the SSSGD_DQNN algorithm for melanoma detection, Section 5 discusses the results and performance evaluation, and Section 6 concludes the research work, summarizing key findings, implications and future directions.

2. Related Works

Akbulut *et al*. [2] created a mobile health app using Convolutional Neural Network (CNN) to aid melanoma diagnosis, despite discomfort. The app analyzes moles, provides rapid results, and displays confidence rates. However, it lacks dataset expansion and benchmarking models.

Kalwa *et al*. [12] created a smartphone app for melanoma diagnosis using image capture, preprocessing, and segmentation. The app uses support vector machine classifiers and adaptive algorithms for reliable results. However, improvements include optimizing thresholding algorithms and exploring color space parameters.

Abbas *et al*. [1] developed a deep learning model for skin cancer classification, using image processing and data augmentation techniques. The system improved AM and benign nevus classification, but its main limitation is prolonged training time.

Sadiq *et al*. [18] created a mobile app for melanoma detection using a smartphone camera. The app captures suspicious skin lesions, extracts features, and uses SVM classification. However, it faces limitations like static testing and reduced accuracy.

Shahin *et al*. [19] used 16 convolutional neural network models to classify skin disease categories from 45,000 HAM10000 dataset images, addressing dermoscopy-based diagnosis in resource-limited settings, but relying on high-quality images.

Nambisan *et al*. [15] developed a hybrid classification pipeline using an annotated irregular network database and traditional hand-crafted features from irregular pigment networks. This approach improved melanoma diagnosis accuracy by combining deep learning and traditional image processing, with U-Net++ as the top performer.

Srinivasu *et al*. [20] developed a skin disease identification system using deep learning-assisted MobileNet V2 and Long Short Term Memory (LSTM). This methodology is lightweight computational framework and maintained stateful information for accurate predictions.

Thanka *et al*. [22] developed a hybrid skin cancer identification method, combining VGG16's feature extraction with XGBoost classification strengths. This method counters overfitting and improves model accuracy, but acknowledges the need for hyperparameter calibration. Mobile applications for melanoma diagnosis face technical and clinical challenges, including image quality, lighting conditions, lesion segmentation, and algorithm accuracy. Clinical issues include skin type variability, limited contextual information, and difficulty detecting early-stage melanomas. User-related issues include compliance, limited medical knowledge, and over-reliance on technology. Regulatory and ethical concerns include data privacy, informed consent, and liability. Mobile applications must integrate with healthcare systems and provide continuous updates.

3. System Model of m-Health

The m-Health architecture is a comprehensive framework that integrates various components to provide seamless healthcare services. The m-Health network integrates web services, emergency response systems, and remote monitoring, ensuring secure patient information storage and retrieval. It also incorporates custom devices for real-time data analysis, enhancing patient outcomes and healthcare delivery.

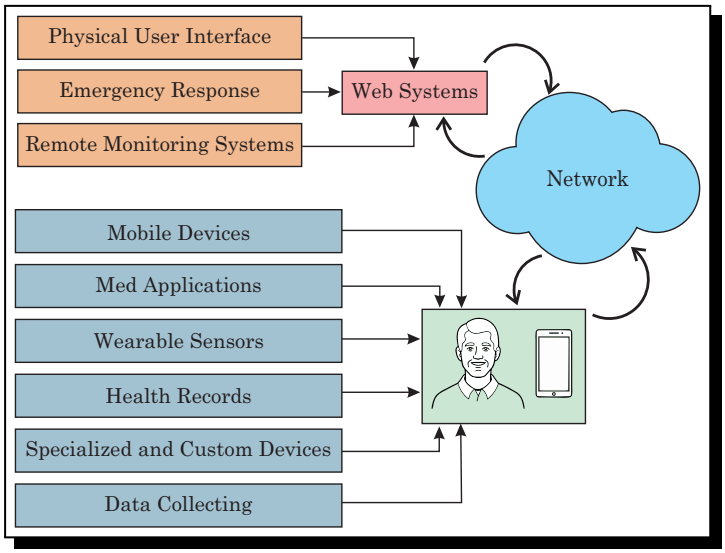

Figure 1. System model of m-Health

4. Proposed Methodology

The SSSGD_DQNN is a machine learning model used for melanoma detection using m-Health. It acquires melanoma images, preprocesses them using the T2FCS filter, segmented them using SGAN, and enhanced dataset diversity through geometric transformations. The model uses Grey Level Co-occurrence Matrices to extract texture features. The trained DQNN accurately classifies images as benign or malignant, facilitating timely clinical intervention. Figure 2 illustrate a model of melanoma detection using SSSGD_DQNNh.

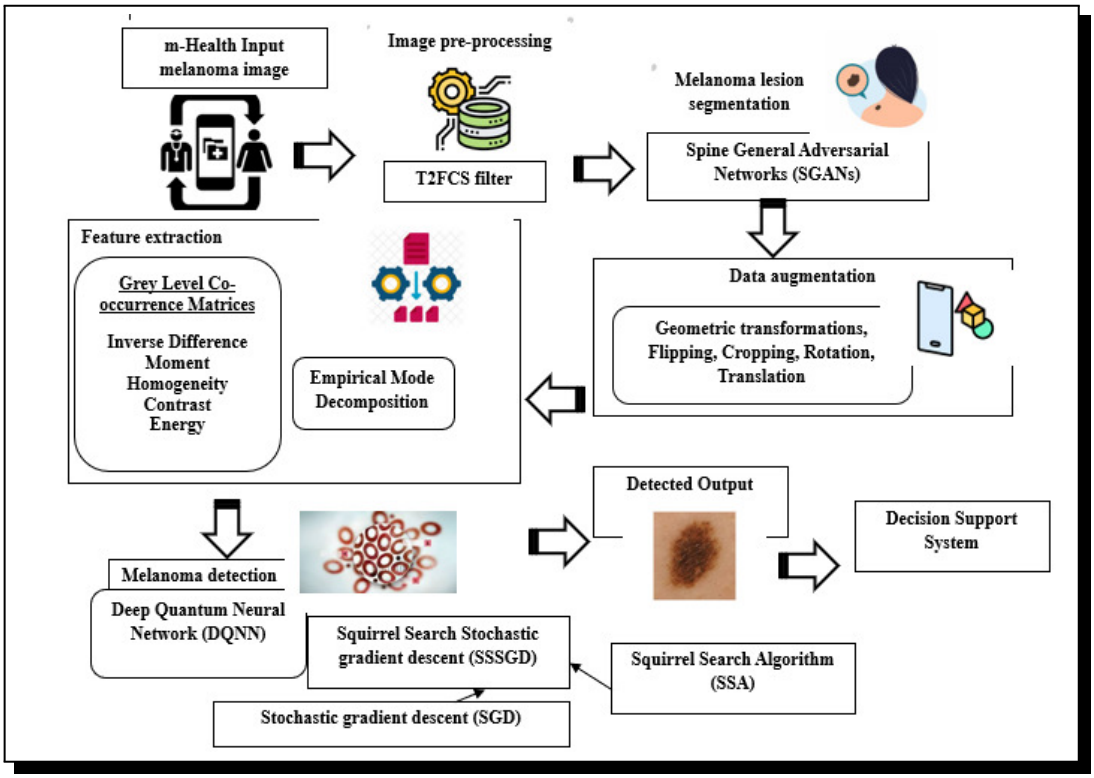

Figure 2. Model of melanoma detection using SSSGD_DQNNh

4.1 *m*-Health Input Image Acquisition

Let examine a dataset P that has t input images, as described below:

$$P = \{D_1, D_2, \ldots, D_h, \ldots, D_t\}, \quad 1 \le h \le t, \tag{4.1}$$

where D_h denotes the input image and t denotes the total number of images. In this case, the pre-processing step receives the input image D_t.

4.2 Pre-Processing

The input image D_t is taken as input for pre-processing process, which is performed using T2FCS filter (Atal [6]). The T2FCS filter is utilized for preprocessing due to its effectiveness in enhancing contrast, reducing noise, and preserving edge information. This adaptive, non-linear filter adapts to image characteristics, handling variability in skin tone and texture, and is robust against noise and artifacts. By improving contrast and reducing noise, T2FCS enables better feature extraction for classification, making it a suitable choice for melanoma image preprocessing, outperforming traditional filters like CLAHE, Histogram Equalization, and Gaussian Filter in enhancing image quality and preserving relevant features. T2FCS enhances melanoma images through a 5-step process: fuzzification converts images to grayscale and applies fuzzy membership functions; Type-2 fuzzy set formation defines footprint of uncertainty; contrast stretching transforms pixels using Type-2 fuzzy sets; defuzzification converts fuzzy sets to crisp values; and output yields enhanced images with improved contrast and reduced noise. Key parameters include fuzzification, Type-2 fuzzy set, and contrast stretching parameters. The pre-processed image is represented as L_j, and it is used for further segmentation process.

4.3 Melanoma Lesion Segmentation Using Spine GAN

Here, the pre-processed image L_j is considered as input for melanoma lesion segmentation process based on Spine GAN (Han *et al.* [9]). Spine GAN generates realistic synthetic data, reducing false positives/negatives and increasing diagnostic accuracy. The Spine GAN architecture consists of two interconnected networks: a Segmentation Network, integrating Deep Atrous Convolution Autoencoder (ACAE) for spinal image feature capture and Long Short-Term Memory (LSTM), Recurrent Neural Network (RNN) for modeling pathological relationships, and a Discriminative Network, built with CNN and convolutional layers, generating precise predictions to isolate affected areas from pre-processed images. Figure 3 shows the Spine GAN structure.

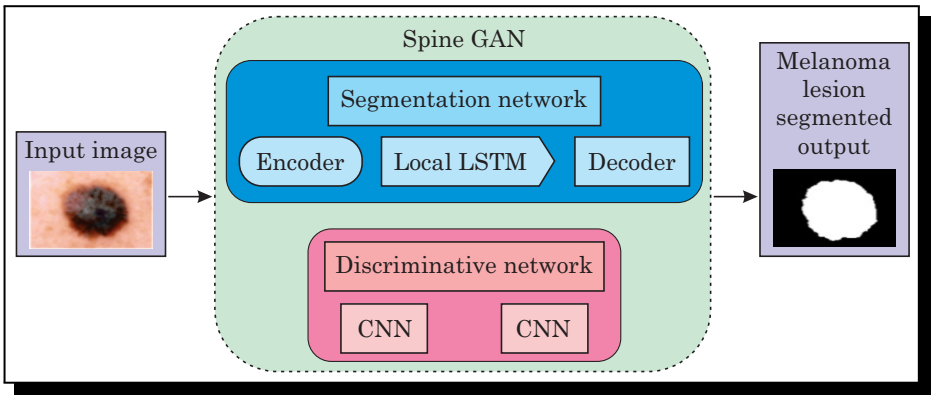

Figure 3. Structure of Spine-GAN

4.4 Data Augmentation

Data augmentation in melanoma detection is crucial because it addresses limitations in dataset size and diversity, enhancing model robustness and accuracy. By generating new training images through techniques, like rotation, flipping, translation, and scaling, data augmentation mitigates overfitting, reduces bias, and improves generalizability. This ensures models can effectively detect melanomas across diverse skin types, lesion shapes, sizes, and orientations, ultimately leading to earlier diagnosis, better treatment outcomes, and improved patient survival rates. Here, the inputted image V_h is given to data augmentation are considered:

(i) *Geometric transformation*: Geometric transformation involves modifying the spatial structure of an image, altering its orientation, shape, and position, without changing its pixel values. This process applies bijective mapping to preserve key geometric properties. Various operations can be applied, such as rotation, flipping, scaling, and translation, to transform the input image. The resulting output denoted as B_1, which retains the original pixel values while exhibiting the modified geometric configuration.

(ii) *Flipping*: Flipping involves rotating an image around its horizontal or vertical axis, where horizontal flip occurs across the vertical axis and vertical flip across the horizontal axis, yielding output B_2.

(iii) *Cropping*: Cropping eliminates unwanted outer regions of an image, trimming peripheral areas to remove extraneous elements, enhance framing, and adjust aspect ratio, resulting in output B_3.

(iv) *Rotation*: Rotation involves circular movement around a central axis, rotating the image clockwise or counterclockwise in a 2D space, producing output B_4.

(v) *Translation*: Image Translation shifts an image horizontally and/or vertically within a 2D space, repositioning it without changing size, shape, or orientation, yielding output B_5. The data augmented output is denoted as $B = B_1, B_2, B_3, B_4, B_5$, and it is utilized for further feature extraction.

4.5 Feature Extraction

Feature extraction is vital for melanoma detection as it identifies relevant patterns and characteristics in dermoscopic images, enabling accurate lesion segmentation, discrimination between benign and malignant lesions, and identification of subtle abnormalities. By extracting key features, such as EMD, and grey level co-occurrence matrix features, like energy, homogeneity, contrast, inverse difference moment can learn to detect melanoma with high accuracy, supporting early detection, improved treatment outcomes, reduced false positives and negatives, and enhanced patient care. Effective feature extraction empowers dermatologists to make informed decisions, ultimately saving lives. Here, the data augment output $B$is taken as input for extracting features.

Gray-Level Co-occurrence Matrix Features

Gray-Level Co-occurrence Matrix (GLCM) features are a type of texture analysis used to extract statistical properties from images. GLCM analyzes the spatial relationships between pixel gray levels, providing valuable information on texture patterns.

4.6 Melanoma Detection using SSSGD_DQNN

Automated detection systems can assist dermatologists, enhance screening, improve patient outcomes, and reduce healthcare costs, ultimately saving lives and reducing healthcare burdens. Hence, after features are extracted, melanoma is detected using an optimized DQNN (Parthasarathy and Bhowmik [17]), trained by SSSGD. As a result, SSSGD enables efficient melanoma detection by leveraging SSA global search capabilities and SGD rapid convergence, resulting in improved accuracy, robustness, and faster convergence in dermatological image analysis. The structure of DQNN is shown in Figure 4.

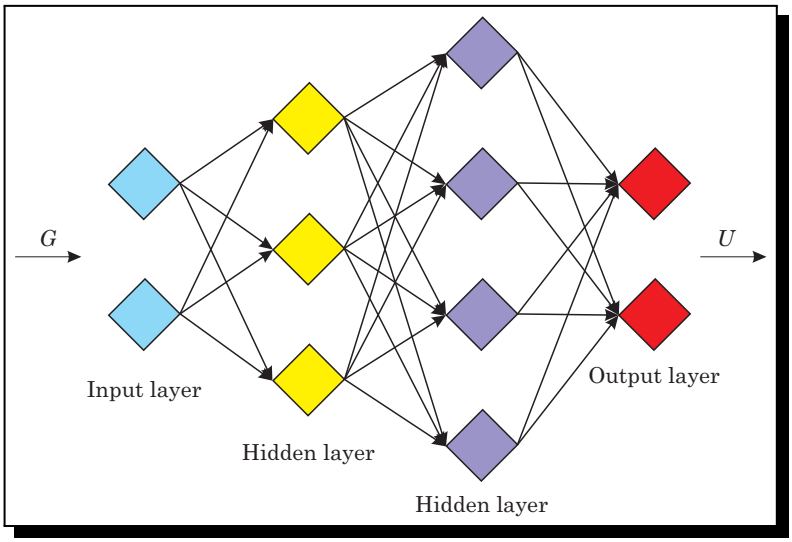

Figure 4. Model of DQNN

SSSGD for Training DQNN

Training of DQNN using SSSGD is crucial for avoiding local minima, improving convergence, enhancing generalization, optimizing weights, and efficiently handling high-dimensional dermatological image datasets. SSSGD combines the strengths of SGD and SSA. SGD[1] particularly mini-batch gradient descent, excels at training deep and complex networks, leveraging added noise to escape local minima. SSA (Jain *et al*. [10]) inspired by squirrel foraging behaviors and gliding locomotion, achieves global optimum solutions with enhanced convergence rates. By integrating global search (SSA) and local search (SGD) capabilities, SSSGD accelerates convergence, promotes robust feature learning, and reduces overfitting, leading to faster, more accurate, and reliable melanoma detection. The steps of the SSSGD are described below:

Initialization: Let look at the n number of flying squirrels H in the forest. The flying squirrel's principal location is shown by,

$$IC_j = ic_S + P(0,1) \times (IC_P - IC_S), \tag{4.2}$$

where $P(0,1)$ is a uniformly distributed random integer between 0 and 1, IC_j is the flying squirrel's position, IC_P is its upper bound, and IC_S is the lower bound of jth flying squirrels in kth dimensions.

[1]S. Ruder, An overview of gradient descent optimization algorithms, arXiv preprint arXiv:1609.04747, 14 pages, (2016), DOI: 10.48550/arXiv.1609.04747.

Computation of fitness: The optimal solution for melanoma detection is obtained by minimizing the fitness function, where the smallest fitness value represents the optimal solution.

$$MSE = \frac{1}{q}\sum_{i=1}^{q}[U - U^*], \tag{4.3}$$

where U indicates the detected DQNN output, U^* stands for the target output, and q is the total number of image samples

Arrange the IC position: Following fitness computation, squirrel positions IC are sorted in ascending order based on fitness values, with the squirrel having the minimum fitness measure relocated to the hickory nut tree, where foraging behavior is influenced by predator presence, and squirrels adjust their locations according to predator probability μ.

Determine the new solution: Based on squirrel foraging behaviors, three scenarios are defined. When predators are absent, squirrels forage in the forest. If predators are present, squirrels seek hiding positions. Specifically, three cases govern squirrel movement:

Case 1: Squirrels transition from acorn nut trees IC_{vt} to hickory nut trees, generating new positions,

$$IC_{vt}^{t+1} = IC_{vt}^{t} + \tau_u \times R_c(IC_{bt}^{t} - IC_{vt}^{t}). \tag{4.4}$$

Case 2: Normal tree-dwelling squirrels IC_{gt} transition to acorn nut trees, mathematically expressed as eq. (4.5),

$$IC_{gt}^{t+1} = IC_{gt}^{t} + \tau_u \times R_c(IC_{vt}^{t} - IC_{gt}^{t}). \tag{4.5}$$

Case 3: Squirrels in acorn nut trees aim to transition to hickory nut trees,

$$IC_{gt}^{t+1} = IC_{gt}^{t} + \tau_u \times R_c(IC_{bt}^{t} - IC_{gt}^{t}). \tag{4.6}$$

Leveraging SGD to avoid local optima, the update equation of SGD is formulated as,

$$E_n(m+1) = E_n(m) - v\nabla b[E_n(m)], \tag{4.7}$$

$$E_n(m+1) = E_n(m)[1 - v\nabla b], \tag{4.8}$$

$$E_n(m) = \frac{-E_n(m+1)}{[1 - v\nabla b]}, \tag{4.9}$$

where $\nabla b[E_n(m)]$ represents the gradient function and v represents the learning rate.

Let $E_n(m) = IC_{gt}^{t}$ and $E_n(m+1) = IC_{gt}^{t+1}$substitute in eq. (4.10),

$$IC_{gt}^{t} = \frac{-IC_{gt}^{t+1}}{[1 - v\nabla b]}. \tag{4.10}$$

Rewrite eq. (4.11),

$$IC_{gt}^{t+1} = IC_{gt}^{t} + \tau_u \times R_c IC_{bt}^{t} - \tau_u \times R_c IC_{gt}^{t}, \tag{4.11}$$

$$IC_{gt}^{t+1} = IC_{gt}^{t}[1 - \tau_u \times R_c] + \tau_u \times R_c IC_{bt}^{t}. \tag{4.12}$$

Substitute eq. (4.11) into eq. (4.13),

$$IC_{gt}^{t+1} = \frac{-IC_{gt}^{t+1}}{[1 - v\nabla b]}[1 - \tau_u \times R_c] + \tau_u \times R_c IC_{bt}^{t}, \tag{4.13}$$

$$IC_{gt}^{t+1} + \frac{IC_{gt}^{t+1}}{[1 - v\nabla b]}[1 - \tau_u \times R_c] = \tau_u \times R_c IC_{bt}^{t}, \tag{4.14}$$

$$IC_{gt}^{t+1}\left[\frac{[1-v\nabla b]+1-\tau_u\times R_c}{[1-v\nabla b]}\right]=\tau_u\times R_c IC_{bt}^{t}, \tag{4.15}$$

$$IC_{gt}^{t+1}=\tau_u\times R_c IC_{bt}^{t}\times\left[\frac{[1-v\nabla b]}{[1-v\nabla b]+1-\tau_u\times R_c}\right]. \tag{4.16}$$

Eq. (4.16) is the integrated equation of SSG and SSA, where τ_u stands for random gliding distance, IC_{bt} describe the location of the flying squirrel that arrived at the hickory nut tree, t represents the current iteration, $R_c=1.9$, and m is between 0 and 1. At iteration t, IC_{gt}^{t} denotes flying squirrels on regular trees, and at iteration $t-1$, IC_{gt}^{t-1} denotes flying squirrels on normal trees.

Seasonal constant evaluation: The flying squirrel's seasonal constant is calculated using,

$$C_c^t=\sqrt{\sum_{k=1}^{\tau}[IC_{vt,k}^{t}-IC_{bt,k}]^2}. \tag{4.17}$$

Additionally, the projected least seasonal constant value is,

$$C_{min}=\frac{10A^{-6}}{365^{\frac{t}{\left(\frac{t_k}{2.5}\right)}}}, \tag{4.18}$$

where t_k denotes the maximum iteration and t denotes the current iteration. Rearrange those flying squirrels that were unable to find the forest for the best winter food supply at random if the seasonal monitoring condition is met.

Random moving: Flying squirrels are assumed to move randomly, unable to directly locate the hickory nut tree as a food source

Re-check feasibility: The optimal solution is assessed using the fitness measure in eq. (4.3). If a new solution surpasses the previous one, the algorithm updates the previous value with the new solution.

4.7 Decision Support System

A DSS integrates with the Melanoma Detection System, offering personalized recommendations, consultations, treatment options, follow-up care, lifestyle modifications, risk assessment, and patient education, enhancing healthcare decision-making.

5. Results and Discussion

This section presents and interprets the results of the SSSGD_DQNN model, highlighting its performance and efficiency in melanoma detection.

5.1 Experimental Set Up

The experimentation was conducted on a Windows 10 PC with 2 GB RAM, Intel i3 Core processor, and Python programming language, utilizing relevant libraries and frameworks for implementation.

5.2 Dataset Description

The Melanoma Skin Cancer Dataset[2] consists of 10,000 dermatological images ($256 \times 256/512 \times 512$ pixels) for melanoma detection algorithm development. The dataset is balanced (50% melanoma, 50% benign) with binary labeling, and includes lesion type, location and image quality annotations. Images were collected from dermatology clinics.

5.3 Performance Measures

The SSSGD_DQNN model performance is comprehensively evaluated using key metrics.

(i) *Accuracy*: Accuracy measures the proportion of correctly classified images (melanoma or benign) out of total images,

$$Acc = \frac{N^{\text{Positive}} + N^{\text{Negative}}}{N^{\text{Positive}} + N^{\text{Negative}} + W^{\text{Positive}} + W^{\text{Negative}}}, \tag{5.1}$$

where N^{Positive} stands for true positive, W^{Positive} for false positive, N^{Negative} for true negative, and W^{Negative} for false negative.

(ii) *Sensitivity*: Sensitivity measures the proportion of correctly identified melanoma cases out of actual melanoma cases,

$$Sen = \frac{N^{\text{Positive}}}{N^{\text{Positive}} + W^{\text{Negative}}}. \tag{5.2}$$

(iii) *Specificity*: Specificity measures the proportion of correctly identified benign cases out of actual benign cases,

$$Spe = \frac{N^{\text{Negative}}}{N^{\text{Negative}} + W^{\text{Negative}}}. \tag{5.3}$$

(iv) *Loss curves*: The loss curve visually represents the DQNN training process, illustrating the relationship between training loss/error and epochs.

(v) *Receiver Operating Characteristics (ROC) curve*: The ROC curve evaluates the DQNN's classification performance, graphically plotting the True Positive Rate (TPR) against the False Positive Rate (FPR), showcasing its ability to distinguish between melanoma and benign classes.

5.4 Comparative Methodologies

The SSSGD_DQNN performance is benchmarked against prominent methodologies, like SVM (Sadiq *et al*. [18]), XGBoost (Thanka *et al*. [22]), CNN (Akbulut *et al*. [2]), and AlexNet (Abbas *et al*. [1]) using training data and K-Fold cross-validation, ensuring a comprehensive evaluation.

5.4.1 Training Data Analysis

Figure 5 presents a comparative evaluation of the proposed SSSGD_DQNN approach versus existing methodologies (SVM, XGBoost, CNN, AlexNet) across various training data percentages, assessing accuracy, sensitivity, and specificity. Figure 5 illustrates the accuracy-based assessment of the SSSGD_DQNN. The SSSGD_DQNN exhibits exceptional performance in melanoma detection, surpassing existing methodologies (SVM, XGBoost, CNN, AlexNet) in accuracy, sensitivity, and specificity. Notably, it achieves 97.38% accuracy with 60% training

[2]M. H. Javid, *Melanoma Skin Cancer Dataset of 10000 Images*, accessed on October 12, 2024, (2024), URL: https://www.kaggle.com/datasets/hasnainjaved/melanoma-skin-cancer-dataset-of-10000-images.

data, outperforming SVM (76.77%), XGBoost (76.73%), CNN (87.05%), and AlexNet (95.85%) by 20.61%, 20.65%, 10.33%, and 1.53%, respectively. Figure 5 shows the sensitivity-based evaluation of the SSSGD_DQNN. SSSGD_DQNN computes a sensitivity value of 98.13% with 70% of training data, while more conventional approaches such as SVM, XGBoost, CNN, and

AlexNet obtain similar values of 78.05%, 79.95%, 94.56%, and 97.01%. Therefore, the SSSGD_DQNN achieves a performance gain of 20.08%, 18.18%, 3.57%, and 1.12% over the current methods. The specificity achieved by the SVM, XGBoost, CNN, AlexNet, and SSSGD_DQNN with 80% of training data is 78.05%, 79.01%, 79.68%, 95.85%, and 97.15%, respectively. This demonstrates that the SSSGD_DQNN achieved specificity is 19.1%, 18.14 percent, 17.47%, and 1.3 percent greater than the current methods.

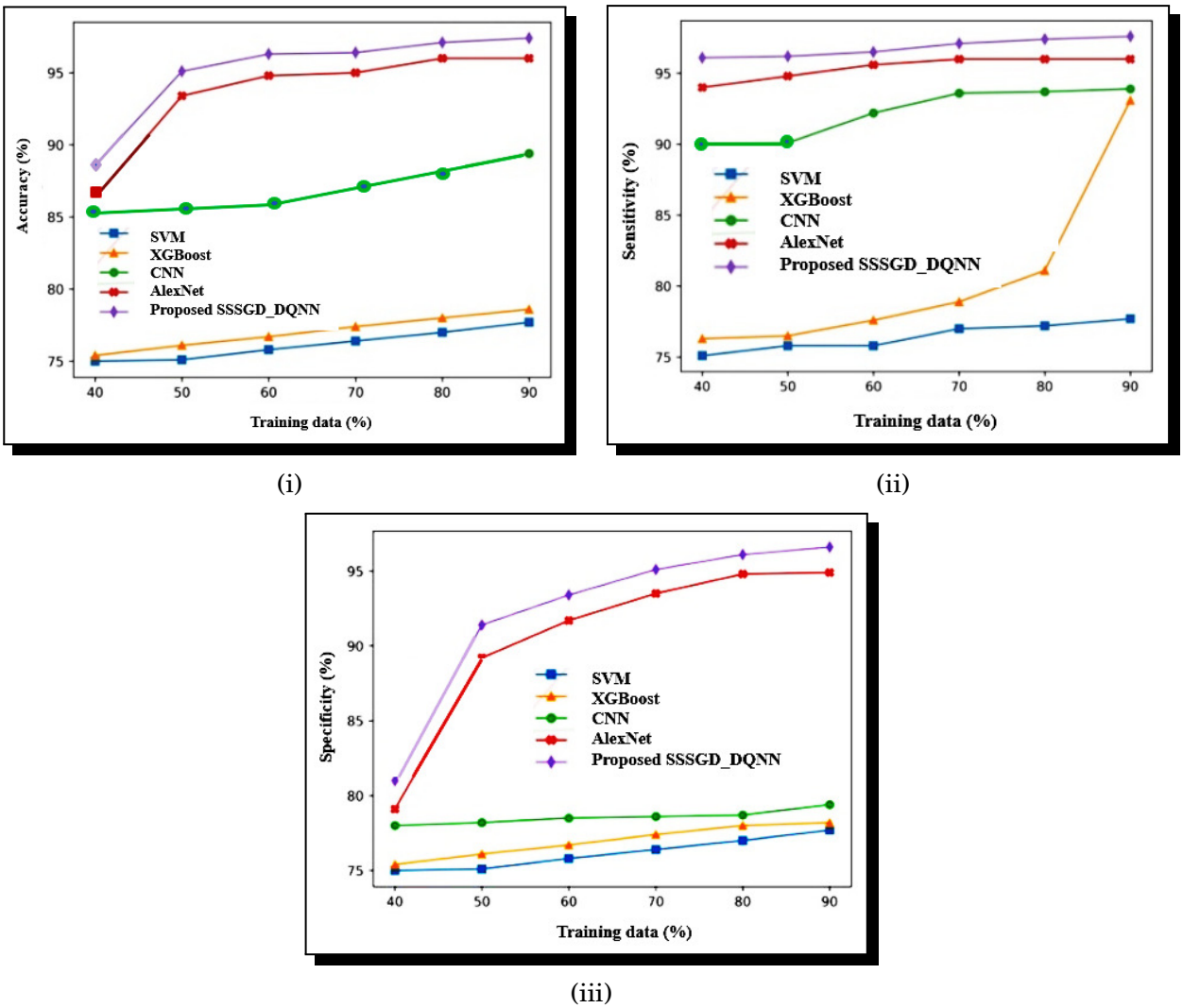

Figure 5. Comparative assessment of SSSGD_DQNN with training data variation: (i) Accuracy, (ii) Sensitivity, (iii) Specificity

This significant improvement validates SSSGD_DQNN effectiveness in melanoma detection, enabling accurate diagnosis, early intervention, and personalized treatment. The comparative analysis underscores SSSGD_DQNN robustness, efficiency, and scalability, making it an ideal candidate for large-scale clinical applications. With its exceptional performance, SSSGD_DQNN

has the potential to revolutionize melanoma detection, reducing false negatives, minimizing biopsy requirements, and enhancing patient outcomes. Furthermore, its adaptability to datasets and real-world applications ensures seamless integration into healthcare systems, paving the way for multicenter trials and continuous refinement. Ultimately, SSSGD_DQNN advancements position it as a transformative tool in melanoma detection, offering healthcare professionals a reliable and efficient solution for improving patient care and saving lives. Its impact extends beyond melanoma detection, contributing to the broader development of AI-driven healthcare solutions and precision medicine initiatives. By harnessing the power of deep learning, SSSGD_DQNN sets a new standard for melanoma detection, inspiring further innovation and advancement in medical imaging analysis.

5.4.2 Loss Curve and Confusion Matrix Analysis

The SSSGD_DQNN performance is evaluated through confusion matrix and loss curve analyses, demonstrating exceptional melanoma detection accuracy, rapid convergence, and substantial decrease in training loss. Table 1 reveals the SSSGD_DQNN exceptional melanoma detection performance, accurately predicting 210 out of 227 outcomes, showcasing high precision and recall.

Table 1. Confusion matrix of the SSSGD_DQNN

Outcomes		Predicted Output	
		No	Yes
Actual output	No	TN = 110	FP = 10
	Yes	FN = 7	TP = 100

Figure 6 illustrates the SSSGD_DQNN rapid learning capability, with a significant decrease in training loss across epochs 0-140, demonstrating improved model stability and convergence. These results validate the SSSGD_DQNN effectiveness in melanoma detection, showcasing its potential for clinical applications.

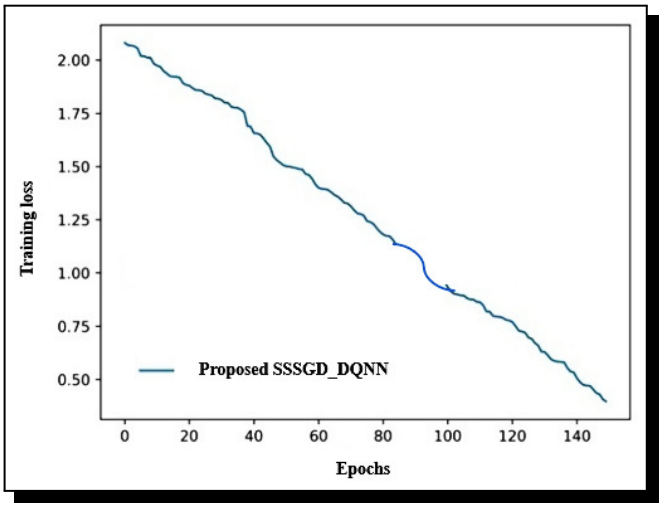

Figure 6. Loss curve of the DQNN used in the SSSGD_DQNN

6. Conclusion

The paper presents a melanoma detection system using SSSGD_DQNN, a cutting-edge *m*-health technology. The system integrates advanced preprocessing techniques, SGAN, geometric transformations, Grey Level Co-occurrence Matrices, and DQNN trained by SSSGD. It achieves exceptional accuracy with a high sensitivity and specificity value. However, limitations include limited dataset diversity, dependence on high-quality image input, potential overfitting, and computational resource intensity.

Competing Interests

The author declares that he has no competing interests.

Authors' Contributions

The author wrote, read and approved the final manuscript.

References

[1] Q. Abbas, F. Ramzan and M. U. Ghani, Acral melanoma detection using dermoscopic images and convolutional neural networks, *Visual Computing for Industry, Biomedicine, and Art* **4**(25) (2021), article number 25, DOI: 10.1186/s42492-021-00091-z.

[2] A. Akbulut, S. Desouki, S. A. Khaliq, L. Khantomani and C. Catal, Design and implementation of a deep learning-empowered *m*-Health application, *Multimedia Tools and Applications* **83**(12) (2024), 35995 – 36011, DOI: 10.1007/s11042-023-17041-x.

[3] K. Aljohani and T. Turki, Automatic classification of melanoma skin cancer with deep convolutional neural networks, *AI* **3**(2) (2022), 512 – 525, DOI: 10.3390/ai3020029.

[4] H. Alquran, I. A. Qasmieh, A. M. Alqudah, S. Alhammouri, E. Alawneh and A. Abughazaleh, The melanoma skin cancer detection and classification using support vector machine, in: *Proceedings of the 2017 IEEE Jordan Conference on Applied Electrical Engineering and Computing Technologies* (*AEECT*) (Aqaba, Jordan, 2017, pp. 1 – 5), (2017), DOI: 10.1109/AEECT.2017.8257738.

[5] R. L. Araújo, R. de A. L. Rabêlo, J. J. P.C. Rodrigues and R. R. V. e Silva, Automatic segmentation of melanoma skin cancer using deep learning, in: *Proceedings of the 2020 IEEE International Conference on E-health Networking, Application & Services* (*HEALTHCOM*) (Shenzhen, China, 2021, pp. 1 – 6), (2021), DOI: 10.1109/HEALTHCOM49281.2021.9398926.

[6] D. K. Atal, Optimal deep CNN–based vectorial variation filter for medical image denoising, *Journal of Digital Imaging* **36**(3) (2023), 1216 – 1236, DOI: 10.1007/s10278-022-00768-8.

[7] C. Barata, M. E. Celebi and J. S. Marques, A survey of feature extraction in dermoscopy image analysis of skin cancer, *IEEE Journal of Biomedical and Health Informatics* **23**(3) (2018), 1096 – 1109, DOI: 10.1109/JBHI.2018.2845939.

[8] C. C. Darmawan, G. Jo, S. E. Montenegro, Y. Kwak, L. Cheol, K. H. Cho and J.-H. Mun, Early detection of acral melanoma: A review of clinical, dermoscopic, histopathologic, and molecular characteristics, *Journal of American Academy of Dermatology* **81**(3) (2019), 805 – 812, DOI: 10.1016/j.jaad.2019.01.081.

[9] Z. Han, B. Wei, A. Mercado, S. Leung and S. Li, Spine-GAN: Semantic segmentation of multiple spinal structures, *Medical Image Analysis* **50** (2018), 23 – 35, DOI: 10.1016/j.media.2018.08.005.

[10] M. Jain, V. Singh and A. Rani, A novel nature-inspired algorithm for optimization: Squirrel search algorithm, *Swarm and Evolutionary Computation* **44** (2019), 148 – 175, DOI: 10.1016/j.swevo.2018.02.013.

[11] A. Javaid, M. Sadiq and F. Akram, Skin cancer classification using image processing and machine learning, in: *Proceedings of the 2021 International Bhurban Conference on Applied Sciences and Technologies* (*IBCAST*) (Islamabad, Pakistan, 2021, pp. 439 – 444), (2021), DOI: 10.1109/IBCAST51254.2021.9393198.

[12] U. Kalwa, C. Legner, T. Kong and S. Pandey, Skin cancer diagnostics with an all-inclusive smartphone application, *Symmetry* **11**(6) (2019), 790, DOI: 10.3390/sym11060790.

[13] V. Mishra, V. A. Kumar and M. Arora, Deep convolution neural network based automatic multi-class classification of skin cancer from dermoscopic images, in: *Proceedings of the 2021 5th International Conference on Intelligent Computing and Control Systems* (*ICICCS*) (Madurai, India, 2021, pp. 800 – 805), (2021), DOI: 10.1109/ICICCS51141.2021.9432160.

[14] A. Murugan, S. A. H. Nair and K. P. S. Kumar, Detection of skin cancer using SVM, random forest and kNN classifiers, *Journal of Medical Systems* **43**(8) (2019), article number 269, DOI: 10.1007/s10916-019-1400-8.

[15] A. K. Nambisan, A. Maurya, N. Lama, T. Phan, G. Patel, K. Miller, B. Lama, J. Hagerty, R. Stanley and W. V. Stoecker, Improving automatic melanoma diagnosis using deep learning-based segmentation of irregular networks, *Cancers* **15** (2023), 1259, DOI: 10.3390/cancers15041259.

[16] S. B. Nasr, I. Messaoudi, A. E. Oueslati and Z. Lachiri, Identification of SNP mutations linked to melanoma via a CNN network: Application to the FGFR2 gene, in: *Proceedings of the 2022 IEEE Information Technologies & Smart Industrial Systems* (ITSIS) (Paris, France, 2022, pp. 1 – 6), (2022), DOI: 10.1109/ITSIS56166.2022.10118421.

[17] R. Parthasarathy and R. T. Bhowmik, Quantum optical convolutional neural network: A novel image recognition framework for quantum computing, *IEEE Access* **9** (2021), 103337 – 103346, DOI: 10.1109/ACCESS.2021.3098775.

[18] M. U. Sadiq, D. Sankalpa, K. Ahfid, A. Sagahyroon and S. Dhou, Preliminary melanoma detection mobile application using support vector machine classification, in: *Proceedings of the 2020 International Conference on Computing, Electronics & Communications Engineering* (iCCECE) (Southend, UK, 2020, pp. 115 – 118), (2020), DOI: 10.1109/iCCECE49321.2020.9231259.

[19] M. Shahin, F. F. Chen, A. Hosseinzadeh, H. K. Koodiani, A. Shahin and O. A. Nafi, A smartphone-based application for an early skin disease prognosis: Towards a lean healthcare system via computer-based vision, *Advanced Engineering Informatics* **57** (2023), 102036, DOI: 10.1016/j.aei.2023.102036.

[20] P. N. Srinivasu, J. G. SivaSai, M. F. Ijaz, A. K. Bhoi, W. Kim and J. J. Kang, Classification of skin disease using deep learning neural networks with MobileNet V2 and LSTM, *Sensors* **21**(8) (2021), 2852, DOI: 10.3390/s21082852.

[21] D. N. H. Thanh, V. B. S. Prasath, L. M. Hieu and N. N. Hien, Melanoma skin cancer detection method based on adaptive principal curvature, colour normalisation and feature extraction with the ABCD rule, *Journal of Digital Imaging* **33**(3) (2020), 574 – 585, DOI: 10.1007/s10278-019-00316-x.

[22] M. R. Thanka, E. B. Edwin, V. Ebenezer, K. M. Sagayam, B. J. Reddy, H. Günerhan and H. Emadifar, A hybrid approach for melanoma classification using ensemble machine learning techniques with deep transfer learning, *Computer Methods and Programs in Biomedicine Update* **3**(2023), 100103, DOI: 10.1016/j.cmpbup.2023.100103.

[23] M. H. Trager, L. J. Geskin, F. H. Samie and L. Liu, Biomarkers in melanoma and non-melanoma skin cancer prevention and risk stratification, *Experimental Dermatology* **31**(1) (2022), 4 – 12, DOI: 10.1111/exd.14114.

[24] M. R. Thanka, E. B. Edwin, V. Ebenezer, K. M. Sagayam, B. J. Reddy, H. Günerhan and H. Emadifar, A hybrid approach for melanoma classification using ensemble machine learning techniques with deep transfer learning, *Computer Methods and Programs in Biomedicine Update* **3** (2023), 100103, DOI: 10.1016/j.cmpbup.2023.100103.